Enrichment of CD56dimKIR+CD57+ highly cytotoxic NK cells in tumor infiltrated lymph nodes of melanoma patients

Published in final edited form as:
Nat Commun. ; 5: 5639. doi:10.1038/ncomms6639.

Enrichment of CD56^{dim}KIR+CD57+ highly cytotoxic NK cells in tumor infiltrated lymph nodes of melanoma patients

Talib Hassan Ali[#1,2], **Simona Pisanti**[#3,4], **Elena Ciaglia**[#3,4], **Roberta Mortarini**[5], **Andrea Anichini**[5], **Cinzia Garofalo**[1], **Rossana Tallerico**[1], **Mario Santinami**[5], **Elio Gulletta**[1], **Caterina Ietto**[1], **Mario Galgani**[6], **Giuseppe Matarese**[3,7], **Maurizio Bifulco**[3,4], **Soldano Ferrone**[8], **Francesco Colucci**[9], **Alessandro Moretta**[10], **Klas Kärre**[11], and **Ennio Carbone**[*,1,11]

[1]Department of Experimental and Clinical Medicine “G. Salvatore”, University of Catanzaro ‘Magna Graecia’, Catanzaro, 88100, Italy

[2]Department of Microbiology, College of Medicine, University of Thi-Qar, Nasseriah, 64001, Iraq

[3]Department of Medicine and Surgery, University of Salerno, Baronissi Campus, Baronissi, 84081, Italy

[4]Department of Pharmacy, University of Salerno, Fisciano,84084, Italy

[5]Human Tumors Immunobiology Unit, Department of Experimental Oncology and Molecular Medicine (R.M. and A.A.), and Melanoma and Sarcoma Unit, Department. of Surgery (M.S.), Fondazione IRCCS Istituto Nazionale dei Tumori, Milan, 20133, Italy

[6]Istituto di Endocrinologia e Oncologia Sperimentale, IEOS-CNR, c/o Dipartimento di Medicina Molecolare e Biotecnologie Mediche, Università di Napoli Federico II, Napoli, 80131, Italy

[7]IRCCS Multimedica, Milano, 20099, Italy

[8]Department of Surgery, Harvard Medical School, Boston, Massachussets, 02115, USA

[9]Department of Obstetrics and Gynaecology, University of Cambridge Clinical School, NIHR Cambridge Biomedical Research Centre, Cambridge,CB2 OXY, UK

[10]Lab. of Molecular Immunology, Department of Experimental Medicine, University of Genova, Genova, 16126, Italy

[11]Department of Microbiology Tumor and Cell Biology, Karolinska Institute, Stockholm, 171 77, Sweden

[#] These authors contributed equally to this work.

Abstract

An important checkpoint in the progression of melanoma is the metastasis to lymph nodes. Here, to investigate the role of lymph node NK cells in disease progression, we analyze frequency,

[*]correspondence to: ennio.carbone@ki.se.
Authors Contribution: T.H.A.; S.P. and E.C. performed the experiments and analyses. R.M and M.S. performed experiments sampling collection, A.A. analyses and data interpretation, manuscript writing. C.G., R.T., E.G., C.I., M.G. performed experiments. M.B., S.F., A.M., K.K. F.C. data analyses and manuscript writing. E.C conceived the study, wrote the manuscript and designed the experiments. All authors analyzed and interpreted the data and critically read the manuscript.

Competing financial interests: The authors declare no competing financial interests.

Europe PMC Funders Author Manuscripts

phenotype and functions of NK cells from tumor-infiltrated (TILN) and tumor-free ipsilateral lymph nodes (TFLN) of the same patients. We show an expansion of $CD56^{dim}CD57^{dim}CD69+CCR7+KIR+$ NK cells in TILN. TILN NK cells display robust cytotoxic activity against autologous melanoma cells. In the blood of metastatic melanoma patients the frequency of NK cells expressing the receptors for CXCL8 receptor is increased compared to healthy subjects, and blood NK cells also express the receptors for CCL2 and IL6. These factors are produced in high amount in TILN and *in vitro* switch the phenotype of blood NK cells from healthy donors to the phenotype associated with TILN. Our data suggest that the microenvironment of TILN generates and/or recruits a particularly effective NK cell subset.

Introduction

T cell mediated immune responses to melanoma antigens have been documented extensively[1,2]. NK cells contribute to anti-tumor immunity, which is traditionally analyzed using human peripheral blood NK cells[3]. In contrast, the role of NK cells in the progression of melanoma to lymph node metastasis has not been investigated. We therefore set out to analyze and compare NK cell phenotype and responses in tumor infiltrated lymph nodes (TILN), ipsilateral tumor-free lymph nodes (TFLN) and peripheral blood (PBL) in a cohort of stage III-IV melanoma patients. The NK cells in healthy lymph nodes are predominantly $CD56^{bright}$ [1]. The comparative analysis of the lymphocyte subsets from lymph nodes and autologous peripheral blood reveals a perturbation of NK cell subpopulation frequencies in the TILN where the $CD56^{dim}$ CD3− NK cells prevail. The phenotype of the NK cells present in the tumour infiltrated lymph nodes resemble a recently described mature and highly cytotoxic NK subset[4,5]. The TILN associated NK subset is functionally active and mediates a robust anti-melanoma cytotoxicity. Moreover, CXCL8, CCL2 and IL6 dominate the lymph node-tumor environment and patient's peripheral blood NK cells indeed express higher amount of CXCR2 and CCR2. Our study reveals an unexpected cross talk between the tumor niche environment and NK cells and identify a selective anti melanoma response mediated by $CD56^{dim}CD57+CD69+CCR7+KIR+$ NK subset.

Results

Frequency and phenotype of NK cells in melanoma patients

We found roughly two-fold more NK cells within TILN (1.3±0.9% of the total lymphocyte population, n=31) versus TFLN (0.7±0.3%, n=12, P=0.02). We analyzed NK cell subsets in blood and lymph nodes by flow cytometry, using the gating strategy depicted in supplementary figure 1. NK cells can be broadly divided in $CD56^{dim}$ cytotoxic cells, which represent the majority of NK cells in the blood, and in $CD56^{bright}$ cytokine producers, which are the most frequent NK cells in lymph nodes [1]. Interestingly, we found that pattern of distribution of these two subsets was significantly perturbed in the blood as well as in the infiltrated lymph nodes of melanoma patients (Fig. 1a,b). The mean frequency of NK cells in patients' peripheral blood (P-PBL) was 5.4±2.0% (n=10) with a prevalence of the $CD56^{dim}$ subset (56.5%±17.5) over the $CD56^{bright}$ subset (43.5±17.5%) (Fig. 1b); the latter ratio was significantly different from that we and others have found in healthy individuals' PBL[6] (Fig. 1b; H-PBL, $CD56^{dim}$=87.8±6.3%; $CD56^{bright}$=12.2±6.3%, n=3, P<0.001). As to

the lymph nodes, the pattern was now reversed (Fig. 1b); the $CD56^{dim}$ subset prevails in the TILN of all the patients tested ($CD56^{dim}$=55.5±21.5%, n=31, $CD56^{bright}$=44.5±21.5%, $P<0.05$) whereas the $CD56^{bright}$ subset prevailed in TFLN ($CD56^{dim}$=31.7±10.8%, n=31, $CD56^{bright}$=68.3±10.8%, n=12, $P<0.001$) just as they do in lymph nodes of healthy individuals. Thus, NK cell subsets were abnormally distributed in melanoma patients, with the potentially cytotoxic $CD56^{dim}$ NK cells being underrepresented in patients PBL and overrepresented in TILN.

The activation marker CD69 in TILN NK cells was even higher than in peripheral NK cells from both patients and healthy donors (Fig. 1 c, $P \leq 0.005$).

Maturation and activation markers were measured by multiparametric flow cytometric analysis in TILN, TFLN and PBL. Both $CD56^{dim}$ and $CD56^{bright}$ NK cell subsets within TILN showed higher expression of CD57, CD69 and CCR7 whereas CD16 expression was significantly augmented in TILN only in the $CD56^{bright}$ subset (Fig. 1d). The CD57 marker has been recently associated with a late, possibly final stage of NK cell maturation[5]. CD57+ NK cells were 3.4 fold more abundant in TILN (48±17.6%, n=31) than in TFLN (14±4.2%, n=12) (P=0.002). It should be noted that the intensity of CD57 staining of NK cells in TILN was weaker compared to the CD57+ subpopulation in the blood (Fig. 1a). Inhibitory Killer-cell Immunoglobulin-like Receptors (KIRs) control several functions of mature NK cells[7, 8]. In spite of the marked variability in KIR expression by TILN and TFLN NK cell subsets the expression of the two inhibitory KIRs stained by the CD158b-specific mAb KIR2DL2 and KIRDL3 was higher on TILN NK cells than on TFLN NK cells (n=3, P=0.002) (Fig. 1d). In line with these data, the intensity of the staining of TILN NK cells by mAbs that recognize KIR3DL2, KIR2DL1/S1, KIR2DL2/L3/S2, KIR2DL1/S1 and CD94 was higher than that of TFLN NK cells in three representative patients (AMM16, 17 and 18, Supplementary Fig. 2a); the difference was statistically significant ($P<0.005$, for KIR2D, 2DS, 3DL and KIR2DL1/S1; $P<0.05$ for CD94) (Supplementary Fig. 2a and b). There was also a trend towards a higher expression of activating receptors NKG2D, DNAM-1 and Natural Cytotoxicity Receptors (NCR, also known as NKP30, NKP44 and NKP46) on TILN NK cells in seven metastatic melanoma patients (AMM5, 6, 11, 12, 13, 15 and 16). We have previously reported that NCRs and DNAM-1 are key receptors for NK cell recognition of melanoma cells and, in particular, of melanoma cell lines derived from lymph node metastases; the latter are more susceptible to NK cell recognition because they express higher levels of ligands for NCRs[9]. Together these results argue in favour of the possibility that TILN is the site where NK cells preferentially enrich and express receptors (KIR, NCR) and markers of maturation (CD57, $CD56^{dim}$) and activation (CD69) suggestive of a more differentiated effector cell phenotype. Moreover these $CD56^{dim}$ NK cells expressed the lymph node homing chemokine receptor CCR7 (Fig. 1d), suggesting that NK cells actively migrate into the TILN from non-lymphoid tissues and from the circulation. The pattern we observed can be due to migration of already fully mature CD57+ NK cells to the TILN, or to maturation *in situ* of immature NK cells migrated from the periphery to TILN. The reduced proportion of $CD56^{dim}$ cells in the PBL of melanoma patients argues in favor of the former possibility. On the other hand, the low CD57 staining on NK cells in TILN suggests that this subpopulation does not correspond exactly to the CD57 bright NK cells in the blood. In

Europe PMC Funders Author Manuscripts

either scenario, our data suggest that TILN might be an important site for NK cell-mediated immunosurveillance against melanoma metastases.

Analysis of cytokine milieu in TILN and TFLN

To test whether the phenotypical differences between the NK cells resident in TILN and those resident in TFLN were due to different cytokine milieus, we performed transwell co-culture experiments. We observed a strong increment in the percentage of both CD69 and CCR7 expressing cells from TFLN treated with TILN supernatants, reaching very similar levels to TILN NK cells (Fig. 2a); this suggests that TILN supernatants contain soluble factors able to convert the phenotype of TFLN NK cells into a phenotype similar to that of TILN NK cells. Thus, we quantified selected cytokines and growth factors in culture supernatants of lymph node-derived cell suspensions from 0 to 96 hrs. TILN produced more CXCL8 (Fig. 2b) ($P<0.005$, n=3), IL-6, and CCL2 than TFLN (Fig. 2c) ($P<0.05$, n=3). Taken together these results show that TILN have a different cytokine milieu which may account for the peculiar NK cell phenotype observed. The expression of CXCL8 and CCL2 chemokines in TILN suspensions might be an early consequence of target cell recognition by NK cells, which has a low threshold for activation[10]. The production of inflammatory cytokines TNFα and IFN-γ by NK cells, instead, requires stronger activation, which may not be attained in the TILN microenvironment, where tumor and NK cells are exposed to other cytokines and tumor growth factors that may be suppressive. Notably, the autologous melanoma metastasis itself produced detectable amounts of CXCL8, IL-6 and CCL2. To assess the impact of these soluble factors on NK cells phenotype, we treated healthy donors PBL cells with single cytokines or a combination of them (Supplementary Fig. 3). $CD56^{bright}$ was the only cell subset responsive to the combination of all three cytokines since it showed an upregulated expression of CD69, CD57, CD16, CD158 and CCR7 (Fig. 2d). Similar data were obtained using purified NK cells.

The expression of the receptors for CXCL8, CCL2 and IL-6 was compared in healthy donors and melanoma patient's peripheral blood NK cells. The frequency of CXCR2 was significantly higher in the $CD56^{dim}$ compartment in patients' peripheral blood with respect to healthy donors. There was a trend towards higher expression of both CXCR2 and CCR2 in the $CD56^{bright}$ subset in patients' PBL. Noteworthy, no differences were found in T cells compartment between healthy donors and patients. The frequencies of CXCR2 and CCR2 expressing NK cells were higher than T cells with these receptors in patient's peripheral blood. However, only the $CD56^{dim}$ CXCR2 expressing subset and CCR2 $CD56^{bright}$ reached the statistical significance (Fig. 2e).

Therefore, it is conceivable to propose that the presence of metastatic cells lead to a cytokine environment in the patients' lymph node that is dominated by CXCL8, CCL2 and IL-6 (Fig. 2b). These soluble factors may induce *in situ* maturation of $CD56^{bright}$ CD3− NK cells to become more mature and cytotoxic CD57+KIR+CD69+CCR7+ NK cells (Fig. 2d). Moreover, CXCL8 and CCL2 produced by metastatic lymph nodes may recruit CXCR2+/CCR2+ cells among both subsets of circulating $CD56^{bright}$ and $CD56^{dim}$ NK cells (Fig. 2e).

NK cells cytotoxicity from tumor-infiltrated lymph nodes

To directly quantify the anti-tumor activity of patients' NK cell subsets, we measured NK cell cytotoxicity against patients' autologous melanoma cells after short-term cultures. We included NK cells isolated from patients' TILN, TFLN and PBL, as well as NK cells isolated from healthy donor PBL. TILN NK cells showed the highest and TFLN NK cells the lowest cytotoxic activity (Fig. 3a and 3b). Altogether, these data demonstrate that autologous TILN-derived NK cells kill lymph node metastatic melanoma cells more efficiently than autologous TFLN- and PBL-derived NK cells ($P<0.005$, n=6), or allogeneic PBL-derived NK cells from healthy donors ($P<0.005$, n=4).To confirm the cytotoxic potential of NK cells *in vitro*, we used a degranulation assay based on the expression of CD107a. We measured basal CD107a surface expression directly after explanting TILN and TFLN of five melanoma patients (AMM17, 18, 19, 20, 21). In all the patients tested, the expression of CD107a was higher on NK cells from TILN, particularly within the $CD56^{dim}$ cells ($P=0.012$) and the CD57+ NK cells ($P=0.005$) (Fig. 3c). We also measured degranulation in response to K562 erytroleukemia cells, the gold standard target for NK cells. Interestingly, only TILN NK cells were clearly activated to degranulate by K562 pulsing, while the TFLN NK cells were unresponsive (Fig. 3d). To assess whether these highly cytotoxic TILN CD57+CD56+ NK cells maintain proliferative potential, we measured the expression of Ki67, a marker of cycling cells. CD57+CD56+ NK cells contained 6 fold more Ki67+ cycling cells (60.1%±13.4) than CD57-CD56+ NK cells (10.4% ±10.2), thus they can proliferate (Fig. 3e).

Frequency of $CD57+CD56^{dim}$ NK cells in TILN and prognosis

The peculiar phenotype of TILN NK cells and their surprisingly high cytotoxic activity against autologous melanoma cells, prompted us to investigate whether the presence of the $CD57+CD56^{dim}$ subset in TILN would correlate with clinical outcome. The ratios between $CD57+CD56^{dim}$ and $CD57+CD56^{bright}$ cells, normalized on the total NK cells percentage in TILN, showed considerable variability among the 20 melanoma patients' TILN investigated, distributing over a range between 1.0 and 16.9 (Fig. 4a). We thus divided the patients into two groups, one with a ≥6 ratio and the other one with a <6 ratio. Since patients with higher ratio mainly belong to stage III, we stratified the patients according to disease stage (Fig. 4b), and found a trend towards association between overall survival and NK ratio within stage III patients.

Although suggestive of a potential role for lymph node NK cells in clinical outcome, this association must be considered as a preliminary observation, to be tested in a much larger cohort in order to assess whether it is an independent variable. In contrast, there was no such pattern when patients were grouped according to the frequencies of CD57+CD8+CD3+ cytotoxic T cells (Supplementary Fig. 5) or Foxp3+CD25+CD3+ T regulatory cells (Supplementary Fig. 6). The differences in survival cannot be explained by novel therapies for metastatic melanoma such as BRAF inhibitors and anti-CTL4-A or PD1 monoclonal antibodies, since the patients studied here were diagnosed before the introduction of these treatment protocols. We noted that male patients dominated in the group with <6 ratio (10 males *vs* 2 females) but not in the group with >6 ratio (3 males *vs* 3 females), and males have been reported to have a worse prognosis in metastatic melanoma[11]. We therefore

cannot exclude gender as a contributing factor in the clinical outcome (Supplementary Table 1).

Discussion

Experimental evidence supports the notion that peripheral blood CD56^{bright} NK cells give rise to CD56^{dim} NK cells which can be further subdivided into subsets on the basis of surface markers and function. CD57 expression is acquired at later stages and marks terminally differentiated cells with high cytolytic activity but very low proliferative potential[5, 6,12]. Under physiological conditions the NK cell population in lymph nodes is dominated by CD56^{bright} cells. We found a striking reversed pattern in tumor infiltrated lymph nodes where most NK cells are CD56^{dim} CD57+. These cells express activation markers and are highly cytotoxic against autologous melanoma cell lines. In view of these findings the ratio between the CD57+CD56^{dim} and the CD57+CD56^{bright}, normalized on the total NK cell percentage in TILN, could represent a valid index of terminal differentiation toward fully competent and highly cytotoxic NK cells. It is remarkable that despite the presence of T_{reg} cells (Supplementary Fig. 4), these KIR+CD57+ NK cells are activated, as demonstrated by the expression of CD69 and their ability to readily degranulate. The high functional activation status of TILN NK cells can even be further increased by *ex vivo* exposure to tumor cells such as K562 cells, despite the possible tolerogenic environment. However, it should be noted that the TILN milieu is characterized by considerable IL-6 production (Fig. 2b), known to drive CD4 T-cell differentiation away from T_{reg} function even in the presence of TGF-β[13]. Noteworthy, melanoma metastases produce CXCL8 [14] and the senescent melanoma cells secrete IL-6, CCL2 and CXCL8 [15]. The serum concentration of CXCL8 increases during melanoma progression[16]. Thus, NK cells may be specifically recruited from the blood to the melanoma infiltrated lymph nodes using the combination of receptors that facilitate homing (CCR7 and CXCR2) and tumor targeting (CXCR2 and CCR2).

The described results suggest that the ratio between CD56dim CD57+and CD57+CD56bright cells in TILN is biologically important and this preliminary observation should be further explored as a prognostic marker in metastatic melanoma. One possible mechanistic/causal scenario that emerges from this observation is that during the progression of malignant melanoma to lymph nodes' metastasis, CD56^{dim}/CD57+ NK cells become enriched in infiltrated lymph nodes, either by selective recruitment or by expansion (or a combination of the two). These NK cells then act to limit further spread. It is however also possible that the differential reactivity patterns in the TILN represent consequence rather than cause of differential tumor progression. For example, association with prognosis might be explained by the ability of particularly aggressive tumors to prevent the enrichment of the fully differentiated NK cell subset. These and other aspects of lymph node NK cell reactivity would be interesting to analyze further in a larger cohort of patients.

To our knowledge this is the first report demonstrating that CD56^{dim} CD57+NK cells can be found in lymph nodes. It will be interesting to investigate how this subpopulation relates to 'memory' NK cells that expand after CMV infection in mice and humans[17, 18]. Besides shedding light on the role of NK cells in tumor protection, our data suggest that TILN NK

Europe PMC Funders Author Manuscripts

cells should be considered as interesting candidate for the design of new adoptive immunotherapy protocols. Lymph nodes explanted during common clinical practice may be a good source of proliferating and highly cytotoxic NK cells that can be expanded *ex vivo* and subsequently administered to patients.

Materials and Methods

Isolation of lymphocytes and melanoma cell cultures

Lymphocytes and melanoma cells were isolated from surgically removed tumor-invaded lymph nodes (TILN) and ipsilateral tumor-free lymph nodes (TFLN) of AJCC stage IIIc or IV melanoma patients. Patients were admitted to Fondazione IRCCS Istituto Nazionale dei Tumori, Milan, Italy. Patients had no history of previous chemotherapy or immunotherapy. All the lesions were histologically confirmed to be cutaneous malignant melanomas. Written informed consent was obtained from all patients in accordance with the Declaration of Helsinki to the use of human biological samples for research purposes. Lymphocytes from TILN of 38 patients (named with the acronym AMM and numbered from 1 to 56), TFLN, and melanoma cells from TILN, were isolated by mechanical disaggregation of surgical specimens. Briefly, tumor specimens were placed in RPMI 1640 (Lonza Verviers, Belgium) supplemented with antibiotics penicillin and streptomycin (Lonza) and minced into 1-2 mm^3 fragments by surgical scalpels. Further tissue disaggregation was achieved by forcing fragments through a metallic mesh with the aid of a sterile siringe plunger. After centrifugation the cell suspension was treated with trypsin (Lonza) and DNAase (Sigma) for 2 min at room temperature to remove dead cells. After two washes and centrifugation, different aliquots of the cell suspensions were used for cryopreservation, for deriving tumor cell cultures and for isolation of lymphocytes. Melanoma cell lines were established by culture of cell suspensions in 25 cm^2 tissue flasks in RPMI 1640 supplemented with 2% glutamine (200mM, Invitrogen), penicillin (100 U/ml), and streptomycin (100 μg/ml) and 10% heat-inactivated fetal calf serum (FCS, Biological Industries), at 37°C in humidified CO_2 atmosphere. Melanoma cell lines were routinely tested for the absence of Mycoplasma contamination by a PCR-based kit (PromoCell). SP11-763.74[19] and SP11-TP61.5[20] mAbs that recognize specific melanoma markers were used to validate histologically primary melanoma cell lines derived from individual patients. The human melanoma metastatic cell lines were grown for not more than 9-10 *in vitro* passages. Lymphocytes from TILN-derived cell suspensions were isolated by Ficoll-Paque (Biopaque) gradient separation.

Isolation of NK cells from short-term TILN and TFLN cultures

NK cells were purified from TILN and TFLN cell suspensions in selected experiments, using the NK cell Isolation kit negative selection and VarioMACS (Miltenyi Biotec) according to the manufacturer's instructions for the depletion of non-NK cells. Briefly, after thawing, TILN and TFLN cell suspensions in RPMI 1640 medium were cultured overnight at 37°C in a 5% CO_2 humidified atmosphere. After a preliminary passage through a Ficoll column (Biopaque) to remove debris and dead cells, the purity of NK cell preparations, determined by cytofluorometric analysis, was above 95%. Freshly enriched NK cells were suspended in IMDM culture medium (Life Technology) supplemented with Penicillin (100 IU/ml) and Streptomycin (100 μg/ml), 10% FBS (Invitrogen). Peripheral blood lymphocytes

(PBL) were isolated from blood of patients with melanoma or of healthy donors by density gradient centrifugation over Ficoll-Paque (Biopaque).

Antibodies

Q66 (KIR3DL2)/IgM (at 1:5 dilution), Z27 (KIR3DL1/S1)/IGg1 (at 1:10 dilution), GL183 (KIR2D2/3/S2)/IgG1 (at 1:20 dilution), XA185 (CD94)/IgG1 (at 1:20 dilution), Z 270 (NKG2A) IgG1(at 1:5 dilution) supernatants produced in our laboratory (A.M.). FITC-antiCD57/IgM (322306 at a 1:100 dilution), PE-antiCD57/IgM (322312 at a 1:100 dilution), PerCP/Cy5.5-CD3/IgG1 (344807 at a 1:100 dilution) PE-antiKi67/IgG1 (350503 at a 1:50 dilution), PE/Cy5 anti-human CD56/IgG2a (304608 at a 1:100 dilution), APC-antiCD3/IgG2a (317317 at a 1:100 dilution), PE-antiFoxp3 /IgG1(320007 at a 1:100 dilution), PE-antiNKp44/IgG1 (325108 at a 1:100 dilution), PE-antiNKp30 IgG1 (325208 at a 1:100 dilution), PE-antiNKp46 IgG1 (331908 at a 1:100 dilution), PE-antiDNAM1/IgG1(338305 at a 1:100 dilution) and PE-antiNKG2D/IgG1(320806 at a 1:200 dilution), PE-antiCCR7/IgG2a (353204 at a 1:100 dilution), PE-antiCD16/IgG1 (302008 at a 1:300 dilution), FITC-antiCD69/IgG1 (310904 at a 1:100 dilution) were from BioLegend. FITC-antiCD3/IgG1 (11-0036 at a 1:100 dilution) and APC-antiCD3/IgG1 (11-0036-42 at a 1:100 dilution) were from eBioscience. PE-Cy7-antiCD56/IgG1 (560916 at a 1:100 dilution), PE-CD69/IgG1 (341652 1:50 dilution) and FITC-CD158b/IgG2b (559784 at 1:50 dilution) were from BD Pharmingen For the cytokines receptors staining on patients and healthy donor lymphocytes, the followed antibodies were used: APC-antiCD126 (IL-6R)/IgG1 (cod.562090 at 1:50 dilution), APC-antiCD182 (CXCR2)/IgG1 (cod.551127 at 1:10 dilution), APC-antiCD192 (CCR2)/IgG2b (cod.558406 at 1:10 dilution) from Miltenyi Biotec, and 7AAD Staining Solution for the cell viability from BD Pharmingen.

Flow-cytometry analysis

Briefly 2×10^5 cells from the total LN suspension were stained with the indicated antibodies followed by flow cytometric analysis. In the indirect staining method the cells were firstly incubated with an appropriate primary mAb followed by FITC (Sigma) conjugated goat anti-mouse secondary antibody. In all experiments the isotype-matched controls were used to set up the negative values. Cells were fixed in 1% formaldehyde for data analysis. Sample fluorescence was measured by the Fluorescence-Activated Cell Sorter FACSCalibur apparatus (Becton Dickinson) and data were analyzed by using the Cell-Quest software (Becton Dickinson).

For intracellular staining to investigate the percentage of T_{reg} cell, cell pellets were resuspended in PBS with 2% FBS and stained with fluorochrome-conjugated anti-CD4, then fixed with 3% formaldehyde (Sigma) in PBS, permeabilized with PBS with 2% FBS and 0.5% saponin (Sigma), and stained with PE-antiFoxp3 /IgG1.

For Ki67 staining, BD Cytofix/Cytoperm kit was used, according to manufacturer's instructions. Briefly cell pellets were resuspended in PBS with 2% FBS and surface stained with fluorochrome-conjugated anti-CD56, anti-CD57 and anti-CD3, then fixed, permeabilized, and intracellularly stained with PE-Ki67/IgG1.

In the direct staining for the cytokines receptors, cells were firstly incubate with Human serum for 15 minutes and then acquired by a FACS Canto II apparatus (Becton Dickinson). The data were analyzed by Flow-Jo version 7.6.4 software analysis.

Microarray cytokine assay

For cytokine profile analysis, TILN, TFLN and tumor samples of AMM 8,9,16 metastatic melanoma patients were thawed and cultured with complete RPMI 1640 medium. Then 1000 μl of culture supernatant were removed at 0, 12, 24, 48, 96 hrs time points and analyzed by biochip array analyzer with the RANDOX cytokine & growth factors array (CTK) micro array kit, for the simultaneous quantification of interleukin-2 (IL-2), IL-4, IL-6, CXCL8, IL-10, Vascular Endothelial Growth Factor (VEGF), Interferon Gamma (IFN-γ), tumour necrosis factor alfa (TNFα), IL-1α, IL-1β, Monocyte Chemoattractant Protein-1 (MCP/1) and Epidermal Growth Factor (EGF). This assay was performed following the manufacturer's recommended procedure. Beads were read on the Bio-Plex suspension array system. Data were analyzed using Bio-Plex manager software with 5PL curve fitting. The limit of detection for this assay is ≈10 pg/ml (based on detectable signal ±2 SD above background). TGF-β production was evaluated by a specific ELISA kit following manufacturer's instructions (R&D Systems and Biosource International).

Cytotoxicity assay

Purified NK cells from TILN, TFLN, and PBL of melanoma patients or healthy donors were cultured 48hrs in presence of 200 IU of IL2 (Chiron) than used as effectors against related metastatic melanoma in vitro established tumour cells using the fluorescent carboxy-Fluorescein Diacetate c'FDA NK assay. Briefly, the target cells were labeled with c'FDA (Molecular Probes). Target cells were mixed with effector cells at different E: T ratios for 3 hours in 200 μl of RPMI 1640 medium at 37° C in a humidified 5% CO2 incubation. The specific lysis of target cells was calculated as follows: % specific lysis = (CT- TE /CT) ×100 (where CT= mean number of fluorescent target cells in control tubes and TE= mean number of fluorescent cells in target + effectors tubes).

CD107a mobilization assay after K562 pulsing

Freshly enriched lymphocytes from TILN and TFLN cell suspension of metastatic melanoma patients were cultured at 37°C in 5% CO2 to different (4:1, 10:1, and 20:1) effector: target ratio with K562 (ATCC) in the presence of PE-conjugated CD107a/IgG1 antibody (BD Pharmingen) in U bottom 96 well plates. After 1 h, Brefeldin A (5μg/ml, Sigma) was added to cultures for an additional 3 h of incubation. At this time cells were collected, washed with PBS with 2% fetal bovine serum (FBS) stained with anti-CD56 PE-Cy5 (Beckman-Coulter-Immunotech), anti-CD3 FITC (Beckman-Coulter-Immunotech) or alternatively with anti-CD3 APC (BD Pharmingen) and analyzed by flow cytometry.

Statistical analysis

Statistical computations were done using the GraphPad Prism 5.0 software for Windows. Data obtained from multiple experiments are calculated as mean ± SD and analyzed for statistical significance using the 2-tailed Student t-test, for independent groups, or ANOVA

followed by Bonferroni correction for multiple comparisons. P-values less than 0.05 were considered statistically significant. We analyzed survival time after surgery in 20 cancer patients. We considered tumor stage (III and IV) and the CD57+CD56dim/CD57+CD56bright ratio (ratio < 6 and ratio ≥ 6) as potential predictors. The value 6 of the ratio was chosen because it was the best discriminatory cut off value for survival. We obtained survival curves with the Kaplan-Meier product-limit estimator. We tested for differences between groups with the log-rank test. We tested for trend in survival across groups with Cox regression including the groups a numeric covariate. We verified proportionality of the hazards with Schoenfeld's residuals. We tested the association between stage and ratio with the Fisher's exact test. The analyses were performed with Stata version 13 (Statacorp, College Station, TX, USA).

Supplementary Material

Refer to Web version on PubMed Central for supplementary material.

Acknowledgments

This work was supported by:

Associazione Italiana Ricerca Cancro AIRC-IG 10189 and UICC International Cancer Technology Transfer Fellowship (E.C.), AIRC-IG 13312 (M.B.); AIRC-IG 12020 (R.M); AIRC-IG 10643 and special Project 5x1000 n. 992 (A.M.).

The Swedish Cancer Society and The Swedish Research Council. (K.K.)

Associazione Educazione e Ricerca Medica Salernitana (ERMES) (M.B.).

PHS grants RO1CA138188 and RO1CA110249 awarded by the National Cancer Institute (S. F.). Fondazione Italiana Sclerosi Multipla (FISM) n. 2012/R/11, the Ideas Programme from the European Research Council Starting Grant "menTORingTregs" n. 310496 and CNR-Grant "Medicina Personalizzata" (G.M.) AICR and the MRC-UK. (F.C.). T. R. and C.E. were supported by a fellowship from FIRC.

References

1). Parmiani G, Castelli C, Santinami M, Rivoltini L. Melanoma immunology: past, present and future. Curr. Opin. Oncol. 2007; 19:121–127. [PubMed: 17272984]

2). Mukherji B, et al. Clonal analysis of cytotoxic and regulatory T cell responses against human melanoma. J. Exp. Med. 1989; 169:1961–1976. [PubMed: 2471770]

3). Burke S, Lakshmikanth T, Colucci F, Carbone E. New views on natural killer cell-based immunotherapy for melanoma treatment. Trends Immunol. 2010; 31:339–345. [PubMed: 20655806]

4). Lopez-Vergès S, et al. CD57 defines a functionally distinct population of mature NK cells in the human CD56dimCD16+ NK-cell subset. Blood. 2010; 116:3865–3874. [PubMed: 20733159]

5). Björkström NK, et al. Expression patterns of NKG2A, KIR, and CD57 define a process of CD56dim NK-cell differentiation uncoupled from NK-cell education. Blood. 2010; 116:3853–3864. [PubMed: 20696944]

6). Caligiuri MA. Human natural killer cells. Blood. 2008; 112:461–469. [PubMed: 18650461]

7). Joncker NT, Raulet DH. Regulation of NK cell responsiveness to achieve self-tolerance and maximal responses to diseased target cells. Immunol .Rev. 2008; 224:85–97. [PubMed: 18759922]

8). Brodin P, Karre K, Hoglund P. NK cell education: not an on-off switch but a tunable rheostat. Trends Immunol. 2009; 30:143–149. [PubMed: 19282243]

9). Lakshmikanth T, et al. NCRs and DNAM-1 mediate NK cell recognition and lysis of human and mouse melanoma cell lines in vitro and in vivo. J. Clin. Invest. 2009; 119:1251–1263. [PubMed: 19349689]

10). Fauriat C, et al. Regulation of human NK cell cytokine and chemokine production by target cell recognition. Blood. 2010; 115:2167–2176. [PubMed: 19965656]

11). Joosse A, et al. Sex is an independent prognostic indicator for survival and relapse/progression-free survival in metastasized stage III to IV melanoma:a pooled analysis of five European organisation for research and treatment of cancer randomized controlled trials. J. Clin. Oncol. 2013; 31:2337–2346. [PubMed: 23690423]

12). Romagnani C, et al. CD56brightCD16- killer Ig-like receptor- NK cells display longer telomeres and acquire features of CD56dim NK cells upon activation. J. Immunol. 2007; 178:4947–4955. [PubMed: 17404276]

13). Kimura A, Kishimoto T. IL-6: regulator of Treg/Th17 balance. Eur. J .Immunol. 2010; 40:1830–1835. [PubMed: 20583029]

14). Schadendorf D, et al. IL8 produced by human malignant melanoma cells is an essential autocrine growth factor. J. Immunol. 1993; 151:2667–2675. [PubMed: 8360485]

15). Ohanna M, et al. Senescent cells develop a PARP-1 and nuclear factor-kappaB associated secretome PNAS. Genes. Dev. 2011; 25:1245–1261. [PubMed: 21646373]

16). Ugurel S, Rappl G, Tilgen W, Reinhold U. Increased serum concentration of angiogenic factors in malignant melanoma patients correlates with tumor progression and survival. J. Clin. Oncol. 2001; 19:577. [PubMed: 11208853]

17). Foley B, et al. Cytomegalovirus reactivation after allogeneic transplantation promotes a lasting increase in educated NKG2C+ natural killer cells with potent function. Blood. 2012; 119:2665–2674. [PubMed: 22180440]

18). Sun JC, Beilke JN, Lanier LL. Adaptive immune features of natural killer cells. Nature. 2009; 457:557–561. [PubMed: 19136945]

19). Temponi M, et al. Binding parameters and idiotypic profile of the whole immunoglobulin and Fab' fragments of murine monoclonal antibody to distinct determinants of the human high molecular weight-melanoma associated antigen. Cancer Res. 1992; 52:2497–2503. [PubMed: 1373670]

20). Chen ZJ, et al. Human high-molecular-weight melanoma-associated antigen mimicry by mouse anti idiotypic monoclonal antibody TK7-371. Cancer Res. 1991; 51:4790–4797. [PubMed: 1716513]

Europe PMC Funders Author Manuscripts

Europe PMC Funders Author Manuscripts

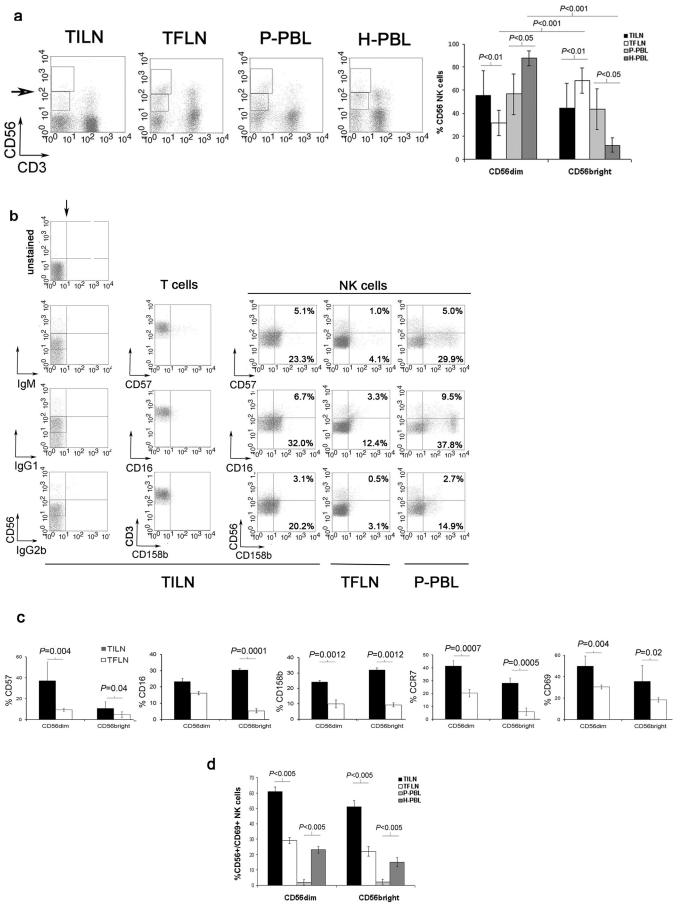

Figure 1. Frequency and phenotype of human NK cells in melanoma patients

(a) Representative example (*left*) for cytofluorimetric analysis of CD56+CD3− NK cell subsets distribution from TILN, TFLN and PBL (P-PBL) in a metastatic melanoma patient in comparison with healthy donor PBL (H-PBL), in the same experimental conditions. Two regions were selected to represent respectively $CD56^{bright}$ and $CD56^{dim}$ populations. Bar graph (*right*) report mean±SD of the frequency of $CD56^{dim}$ and $CD56^{bright}$ NK subsets within TILN (black column, n=31) and TFLN (white column, n=12) gated on lymphocytes of all metastatic melanoma patients tested. In parallel light grey columns show the frequency of $CD56^{dim}$ and $CD56^{bright}$ NK subsets within peripheral blood lymphocytes of patients (P-PBL, n=10) and dark grey columns that of healthy controls (H-PBL, n=3). (b) Expression of CD57, CD16 and CD158b on $CD56^{dim}$ and $CD56^{bright}$ NK cell subsets from TILN, TFLN and P-PBL. Dot plots from one representative patient are presented. The quadrant marker has been set according to the isotype controls; to corroborate the validity of the markers T cells where used as internal negative control in vertical and the bright/dim boundary in horizontal. The identical quadrant marker has been applied on all the plots. (c) Expression of CD57, CD16, CD158b, CCR7, CD69 on $CD56^{dim}$ and $CD56^{bright}$ NK cell subsets. Bar graphs report mean±SD of the percentage of positive cells for each indicated marker in gated NK cells from TILN and TFLN of metastatic melanoma patients (n=12). **(d)** CD69+ CD56+CD3− NK cell subsets frequencies from TILN (n=31), TFLN (n=12), P-PBL (n=10) and H-PBL (n=3). Values shown are the mean±SD of percentages of double positive cells

indicated. In all experiments shown *P* value is calculated by ANOVA followed by post-hoc Bonferroni test.

Europe PMC Funders Author Manuscripts

Europe PMC Funders Author Manuscripts

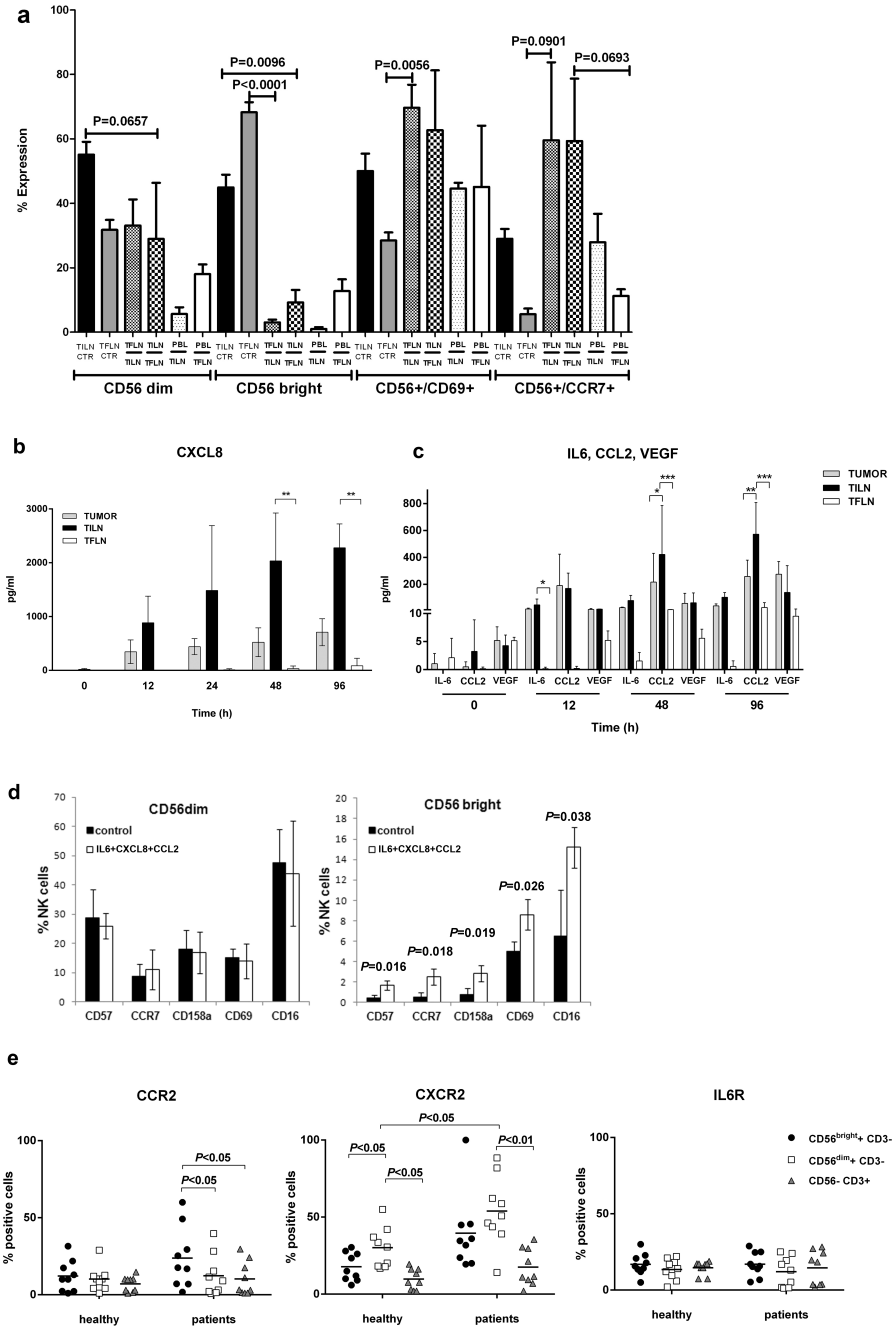

Figure 2. Analysis of cytokine milieau in melanoma infiltrated and tumor free lymph nodes

(a) Transmissible factors' influence on CD56 cell subset frequency and CD69 and CCR7 cell surface expression was evaluated in transwell cocultures. TILN and TFLN samples (n=3) were analysed for CD69 and CCR7 expression within $CD56^{dim}$ and $CD56^{bright}$ NK cell subsets. Each specific bar pattern represents the transwell condition with TFLN, TILN or PBL in the upper chamber of the transwell and TFLN or TILN in the lower one. The bar diagram shows the mean of values ± SD (ANOVA, n=3). **(b, c)** Cytokine production in supernatant of TILN, TFLN and melanoma tumor samples. The histogram reports CXCL8

production by tumor cells (grey column), TILN lymphocytes (black column) and TFLN lymphocytes (white column) as mean±SD of three independent experiments (b). IL-6, CCL2, VEGF release by tumor cells, TILN and TFLN lymphocytes (the results represent mean±SD of three separate experiments, ANOVA) (c). **(d)** The combination of IL6, CXCL8 and CCL2 can influence $CD56^{bright}$ phenotype on CD56+CD3− NK cells derived from peripheral blood of healthy donors. Bars shows the percentage ± SD of $CD56^{dim}$ (*left panel*) and $CD56^{bright}$ (*right panel*) expressing each indicated marker. Results shown are representative of three independent experiments. Statistical analysis is indicated (ANOVA). **(e)** Frequency of NK and T cell subsets ($CD56^{bright}$+CD3−; $CD56^{dim}$+CD3−; CD56-CD3+) expressing the CXCL8 receptor (CXCR2), CCL2 receptor (CCR2) and IL6 receptors in healthy donors (n=8) and melanoma patients peripheral blood (n=9). Each dot represents a different patient or healthy donor. Bars represent mean values. Statistical analysis is indicated (ANOVA).

Europe PMC Funders Author Manuscripts

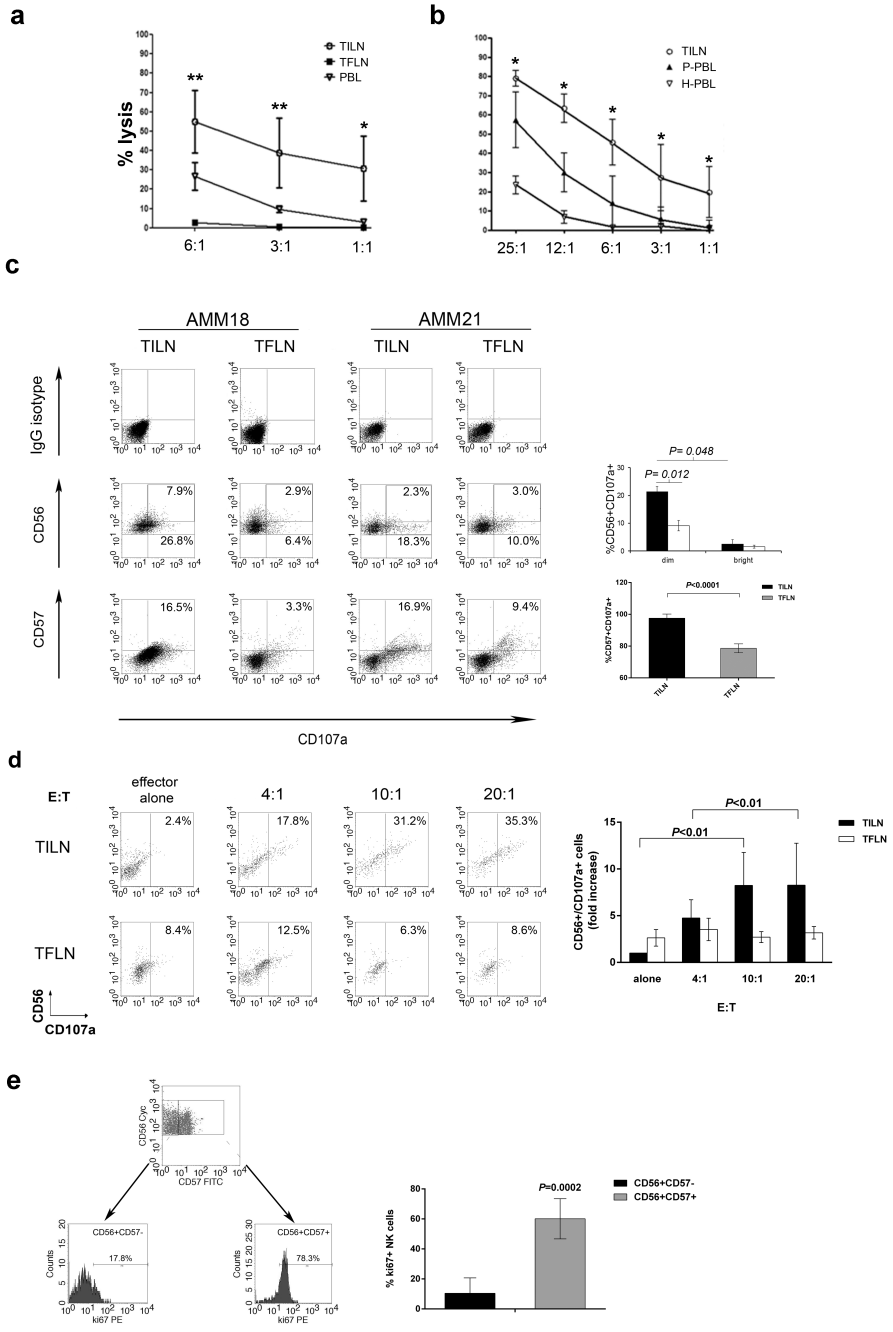

Figure 3. NK cells from tumor-infiltrated lymph nodes have strong cytotoxic potential

(a, b) Cytotoxicity of NK cells against autologous melanoma cell lines. The graph reports the mean percentage specific lysis ±SD of at least 3 individual representative experiments performed at the indicated Effector:Target (E:T) ratios. The figure compares killing by autologous NK cells isolated from patients' TILN (circle symbol) and TFLN (black square) or allogenic NK cells isolated from healthy donors' PBL (H-PBL, black triangle) (a). Comparison between cytotoxicity of autologous NK cells isolated from TILN (circle symbol, n=6), patients' PBL (P-PBL, black triangle, n=4) and allogenic NK cells isolated

from healthy donors' PBL (H-PBL, white triangle, n=4) (b). Statistical analysis is indicated (ANOVA). **(c)** Basal CD107a surface expression on TILN- and TFLN-NK cells from 2 representative (AMM18 and AMM21) patients, as assessed by FACS analysis. Numbers in dot plots indicate the percentage of CD107a positive cells within $CD56^{dim}$ and $CD56^{bright}$ NK subsets (upper panels) or alternatively within CD57+CD56+ NK cells (lower panels). The dot plot quadrants are set according to the isotype IgG control for TILN and TFLN as shown in the figure. In the CD56 dot plots two additional regions identify bright and dim NK cell subsets. The bar diagrams (right) refer to the mean of values ± SD of experiments performed in 5 metastatic melanoma patients (ANOVA). **(d)** Two representative metastatic melanoma patients (AMM17 on the *left* and AMM20 on the *right*) FACS analysis of the CD107a mobilization assay gating on CD56+CD3− TILN and TFLN NK cells after K562 pulsing at different E:T ratios. Quadrants are drawn according to the IgG isotype control for TILN and TFLN, as shown. The bar diagram (right) shows the mean of values ± SD (n=4) expressed as fold increase of CD107a expression in target pulsed NK cells over NK cells alone. **(e)** Ki67 intracellular staining TILN CD57+CD56+ NK. The bar diagram (right) shows the mean of values ± SD (n=5).

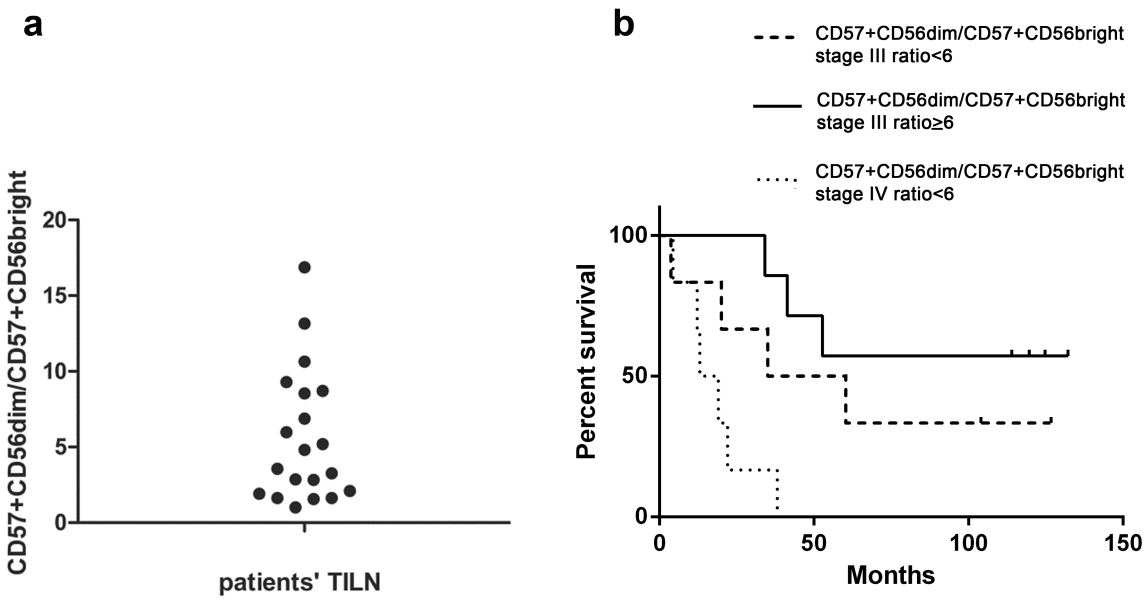

Figure 4. Stratifying by stages patient's survival in groups with high or low frequency of CD57+CD56^{dim} NK cells in tumor-infiltrated lymph nodes

(a) CD57+CD56^{dim}/CD57+CD56^{bright} ratio was calculated as a proportion of total NK cell frequency in the melanoma infiltrated lymph nodes (TILN) of each metastatic melanoma patient. **(b)** Kaplan-Meier survival curves in 7 patients with CD57+CD56^{dim}/CD57+CD56^{bright} ratio≥6 (continuous line), 6 patients with CD57+CD56^{dim}/CD57+CD56^{bright} ratio<6 stage III (dashed line) and with 6 patients CD57+CD56^{dim}/CD57+CD56^{bright} ratio<6 in stage IV (dotted line). The curves were compared with Log Rank Test (P=0.004) and a test for trend ($P=0.00068$).